Ultra Low Phase Noise 16GHz Oscillator Using a Distributed Bragg Resonator

St.John Gilbert, Simon Bale and Jeremy Everard
School of Physics, Engineering and Technology
University of York
York, United Kingdom
stjohn.gilbert@york.ac.uk, simon.bale@york.ac.uk, jeremy.everard@york.ac.uk

***Abstract*—This paper presents the design of a 16GHz oscillator using a high Q distributed Bragg resonator (DBR) with an aperiodic arrangement of high purity, low-loss alumina plates (ϵ_r = 9.75, loss tangent of $\approx 1 \times 10^{-5}$ to 2×10^{-5}). The resonator demonstrates an unloaded Q up to 160,000 & the plates are held in place using Spira-Shield O-Ring gaskets to maintain mechanical stability. Preliminary phase noise measurements of -77dBc/Hz at 100Hz offset & -135dBc/Hz at 10kHz offset are presented.**

***Index Terms*—Distributed Bragg resonator, 16GHz, High unloaded Q, Spira-Shield, Ultra low phase noise**

I. Introduction

The oscillator used in time sensitive electronic equipment sets the ultimate phase noise performance of the system. It is therefore essential to develop ultra-low phase noise oscillators to ensure that phase noise, jitter & Allan deviation are minimised. The phase noise is proportional to $1/Q^2$ [1], [2].

Microwave cavities are often used as the resonant element in oscillators as they are capable of handling high powers but the Q is limited by the surface resistivity of the metal walls. Higher unloaded Qs can be achieved by incorporating low loss dielectric plates into the cavity [3]–[9] that confine the majority of the field energy to the centre section and away from the lossy end walls.

A periodic Bragg resonator was presented by Maggiore *et al* stating an unloaded Q of 531×10^3 [3] at 18.99GHz using sapphire plates.

Flory *et al* [4], [5] have demonstrated periodic sapphire resonators exhibiting unloaded Qs of 650,000 and 450,000 at 9 and 13.2 GHz respectively consisting of interpenetrating concentric sapphire rings and plates inside a metal cavity to reduce the losses in the metal walls. For maximum power reflection in the air/dielectric interface, the thickness of the plates and air sections were a quarter of the wavelength of the guide wave.

It was shown in simulation by Breeze *et al* [6] that distributing more of the field energy in the air gaps than in the dielectric plates by using an aperiodic arrangement, increases the Q factor compared to a periodic DBR. A 30GHz sapphire resonator was later developed by that research group [7] demonstrated an unloaded Q of 600,000.

The authors wish to thank Agilent Technologies Inc (Santa Clara, California) and the UK Engineering and Physical Sciences Research Council (EPSRC) for their funding and support

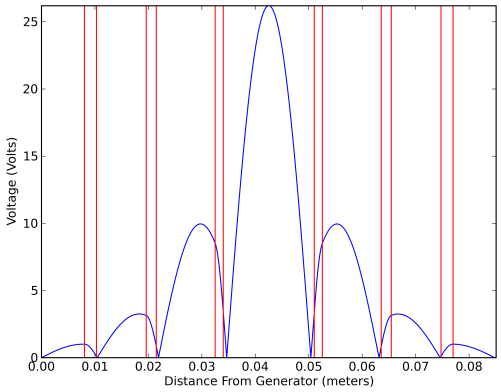

Fig. 1. Simulation voltage standing wave inside a 10GHz DBR developed by this research group [8], the peaks occur in the lower loss air sections, rather than the more lossy dielectric sections. The vertical lines represent the dielectric plates

A 10GHz aperiodic DBR was built at York by Bale and Everard [8], demonstrating a Q_0 of 197,000 where it was also shown in simulation that the unloaded Q of the resonator saturates when 8 plates were used. The simulated voltage standing wave pattern of the aperiodic resonator developed by this research group is shown in figure 1. This shows that the voltage peaks occur in the low loss air sections rather than inside the more lossy dielectric sections (vertical lines), as is the case for a periodic structure.

A tunable 10GHz resonator has also been developed demonstrating insertion loss variance of -2.84 to -12.03dB with unloaded Q varying from 43,800 to 123,000 within a 130MHz tuning range [9] by this research group.

In this paper, the designs and phase noise measurements of a high power and a low power feedback oscillator using a high Q aperiodic DBR operating at 16GHz are presented.

II. Ultra Low Oscillator Phase Noise Theory

It is necessary to develop an equivalent circuit model from which a phase noise equation can be derived. Such a model has been developed by Everard, [1], [2], shown in figure 2, where an equation is derived and expanded to include the flicker

$$L(f) = 10NLog\left(\underbrace{\frac{F_2kT}{C_0 2P_{AVO}}}_{A} + \underbrace{\left(1+\frac{f_C}{\Delta f}\right)}_{B}\left(\frac{F_1kT}{2P_{AVO}}\underbrace{\left(\frac{1}{\left[1-\frac{Q_L}{Q_0}\right]^2}\right)}_{C} + \underbrace{\frac{F_1kT}{8(Q_0)^2\left(\frac{Q_L}{Q_0}\right)^2\left(1-\frac{Q_L}{Q_0}\right)^2 P_{AVO}}}_{D}\left(\frac{f_0}{\Delta f}\right)^2\right)\right) \quad (1)$$

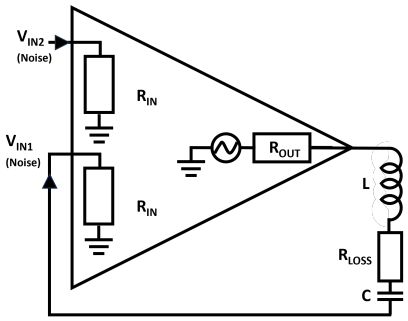

Fig. 2. Equivalent circuit model of the feedback oscillator where the resonant element is modelled as an LCR network and the feedback path is modelled as a two input amplifier [1]

noise corner of the feedback amplifier, the noise outside the resonator 3dB bandwidth and noise from a buffer amplifier. The complete phase noise equation is given in equation 1 [2].

This equation can be split into four sections, where section A is the noise introduced by the buffer amplifier. F_2 is the noise figure of the buffer, C_0 is the coupling ratio between the power available at the resonator input, P_{AVO}, and the power at the input of the buffer. Part B is the flicker noise spectral density of the feedback amplifier where F_C is the flicker noise corner of the device. The noise floor outside the resonator 3dB bandwidth is calculated using part C, caused by the closed loop amplifier gain. Finally, the oscillator phase noise within the 3dB bandwidth is given in part D which is the specific phase noise equation where $R_{OUT} = R_{IN}$ and the power is defined as the power available at the input of the resonator, P_{AVO}.

Part D is minimum when $Q_L/Q_0 = 1/2$, and therefore the insertion loss of the resonator is 6dB. Here the maximum power is dissipated by the resonator [10]. The loop losses must be overcome by the feedback amplifier which should have a low noise figure (F_1) and low flicker noise corner (f_c) such that equation 1 is kept to a minimum. It is also necessary that this amplifier produce high output power and be placed as close to the resonator input as possible so that P_{AVO} is high which also minimises equation 1.

If the open loop phase shift deviates from an integer multiple of 360°, then the oscillator no longer oscillates at the resonant frequency of the resonator. The effective Q of the resonator reduces at a rate proportional to the phase slope of the resonator causing a degradation to the phase noise in the thermal and flicker regions. It is demonstrated experimentally by Cheng and Everard in [11] that the phase error causes a degradation to the phase noise by a factor of $cos^4\theta$, where θ is the open loop phase error.

III. Oscillator Design

A. High Q Distributed Bragg Resonator

The resonant element is a 16GHz Bragg resonator designed to operate in the high Q TE_{011} mode. High purity, low loss alumina plates (ϵ_r = 9.75, loss tangent of $\approx 1 \times 10^{-5}$ to 2×10^{-5}) are distributed within a microwave cavity. The section heights increase towards $\lambda/4$ at the far end of the cavity as demonstrated in figure 1. More energy is reflected away from the lossy end walls resulting in a higher unloaded Q than the classic air filled cavity. The size of each section asymptotically approaches $\lambda_{Guide}/4$ and was designed using the same process adopted in [8], by considering each air/dielectric section as a separate waveguide section. The separate sections were simulated together and optimised using a genetic algorithm to maximise the Q.

Coupling to the resonator is achieved using small coaxial loop probes positioned close to the side wall of the central section orientated in the same direction as the plates. RG405 coax is used for the probes and the diameter of the area enclose by the centre conductor is 0.5mm. A maximum measured unloaded Q of 160,000 was observed although there was large insertion loss of approximately 30dB. The unloaded Q of the resonator used in the final oscillator was 115,000 with an insertion loss of 9.14dB.

B. Amplifiers

Three amplifiers have been used in the oscillators, Analog Devices HMC3653, Marki APM6849SM and an amplifier consisting of 4 APM6849 devices connected in parallel using Rat Race couplers. The parallel amplifier was used to suppress the flicker noise introduced by a single device and to increase the output power. It has been shown by Boudot and Rubiola [12] that a flicker noise reduction of $3log2(m)$ dB is possible by using m number of parallel amplifiers. The measured gain, output power in 1 dB compression, $P_{Out1dBm}$, and noise figure of these amplifiers are shown in table I.

Amplifier	Gain /dB	$P_{Out1dBm}$ /dBm	NF /dB
HMC3653LP3BE	11.637	13.3	6.14
APM6849SM	9.835	19.6	4.89
Parallel APM6849SM	7.41	21.5	6.47

TABLE I
MEASURED AMPLIFIER PARAMETERS AT 16GHZ FROM THREE AMPLIFIERS CONSIDERED SUITABLE FOR USE IN A 16GHZ OSCILLATOR

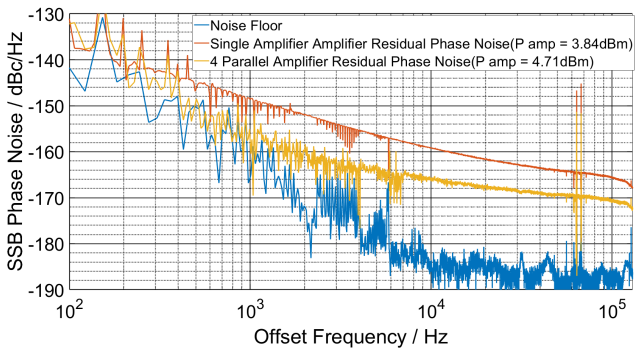

Fig. 3. Measured residual phase noise of the single amplifier, parallel amplifier and noise floor of the measurement system with a resolution bandwidth of 7.63Hz, 7.5dBm input power to the mixer after 10,000 correlations

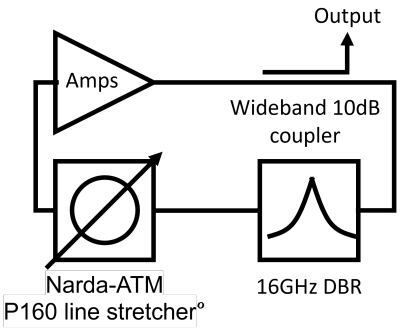

Fig. 4. Generic 16GHz DBR oscillator block diagram, the 'Amps' component represents the different amplifier combinations used in the measurements

The measured gain of the parallel amplifier has decreased by 2.43dB when compared with a single APM6849SM device, and the noise figure has increased by 1.51dB whilst the output power in 1dB compression has only increased by 2dB and not the expected 6dB. It is clear that losses have been introduced by the Rat Race structure in the parallel amplifier.

A residual phase noise measurement of the HMC3653 amplifier was made using an FSWP50 indicating a flicker noise corner of 30kHz. Residual phase noise measurements of the APM6849SM single device and the parallel configuration were made using the cross correlation system developed at York by Bale *et al* [13] to demonstrate the flicker noise suppression. The noise floor of the FSWP was too high to measure the single and parallel APM6849 amplifiers and so Bale's system was used as it has a lower noise floor. 10,000 correlations were carried out and the input power to the mixers, P_{IN}, was kept constant at 7.5dBm.

The measured residual phase noise of both amplifiers is plotted in figure 3 from which the estimated flicker noise corner of the amplifier reduces from 70kHz to 20kHz. The far from carrier noise is estimated to be -166dBc/Hz for the single amplifier and -170dBc/Hz for the parallel amplifiers. This system is only suitable to measure up to 100kHz offsets so an estimate has been made for the amplifier far from carrier noise. Theory predicts a 6dB reduction in flicker noise for four parallel amplifiers. It is estimated from the plotted results and different operating condition that the flicker noise improvement due to the parallel network is between 5-6dB.

IV. Oscillator Phase Noise Measurement, Conclusions and Further Work

At 16GHz the losses introduced by the interconnecting cables, the passive components and the PCB connectors is large and therefore the open loop gain must be increased to overcome this. The high power oscillator consisted of a series combination of two single APM6849 devices followed by the parallel amplifier. A 6dB attenuator was placed between the two single devices to reduce the saturation of the second stage with the aim of reducing any increase in flicker noise and noise figure. However, the cascaded noise figure of the feedback components was calculated to be 25dB which has had a significant affect on increasing the oscillator phase noise.

To reduce the noise figure, a second oscillator was built using two lower power HMC3653 devices. A 6dB attenuator was placed between these devices. The HMC3653 offers increased gain of 11.7dB at 16GHz, therefore fewer devices were required to overcome the loop losses. The noise figure of the feedback path was calculated to be 14dB. In both oscillators, a Narda-ATM P160 line stretcher was used to adjust the loop phase shift and a 10dB wideband coupler designed in house was used to couple the oscillator output.

Phase noise measurements of both oscillators were made using the Rohde and Schwarz FSWP 50 phase noise measurement system and both oscillators were placed in a shielded enclosure for the measurement. 1000 correlations were made in the smallest offset frequency band (1-10Hz) with a 5% resolution bandwidth. The measurement time was approximately 1 hour.

Using equation 1 and the measured parameters of Q_L, Q_0, P_{1dBm}, F_C and calculated cascaded NF, the theoretical oscillator phase noise can be calculated for both the high power and low power configurations. The estimated F_C has been increased to 30kHz in the high power theory plot as 20kHz gave a phase noise calculation that was too small and was therefore inaccurate to what has been measured. This suggests that the saturation of the parallel amplifier has caused an increase to the flicker noise. The measured and theoretical oscillator phase noise plots are shown in figure 5.

The lower power oscillator matches the theory above 100Hz offsets whereas the higher power oscillator measurement is greater than the theory at offsets less than 1kHz. It is thought that the high noise figure and potential excessive saturation of the amplifiers used in the high power oscillator has introduced additional noise components to the phase noise spectrum.

The higher power oscillator is expected to present lower phase noise than the lower power configuration. However, the number of amplifiers required in the high power oscillator and the 6dB attenuator used to limit amplifier suppression has considerably increased the noise figure and therefore increased

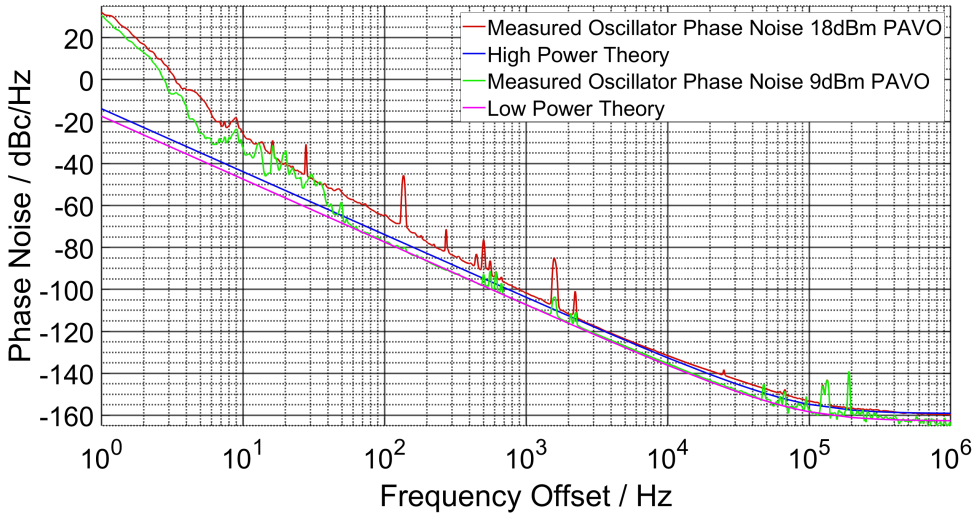

Fig. 5. Theoretical and measured oscillator phase noise plots of the 16GHz DBR oscillator. The theoretical plot is calculated using equation 1 and measured parameters Q_L, Q_0, P_{1dBm}, F_C and NF

the oscillator phase noise such that it is larger than the low power oscillator.

The close to carrier frequency noise increase is possibly due to the oscillation frequency changing during the measurement process as result of thermal effects in the oscillator. The change in oscillator frequency appears as positive phase noise in the measurement at an offset from the initial oscillator frequency. Temperature stabilisation of the resonator should be considered to stop the metal resonator enclosure expanding/contracting and improve the close to carrier phase noise response.

Future iterations of the oscillator should aim to reduce the number of series amplifiers in the feedback loop to reduce the noise figure and saturation of the amplifiers. Further work on resonator coupling to ensure small insertion loss whilst maintaining a high unloaded Q is necessary and alternative methods of coupling should be explored. 20-30dB improvements in phase noise should therefore be possible.

ACKNOWLEDGMENT

The authors wish to thank Agilent Technologies Inc (Santa Clara, California) and the UK Engineering and Physical Sciences Research Council (EPSRC) for their funding and support

REFERENCES

[1] J. Everard, *Fundamentals of RF Circuit Design*, 1st ed. New York, USA: Wiley, 2001.

[2] J. Everard, T. Burtichelov, and K. Ng, "Ultralow Phase Noise 10-MHz Crystal Oscillators," *IEEE Transactions on Ultrasonics, Ferroelectrics, and Frequency Control*, vol. 66, no. 1, pp. 181–191, Jan 2019.

[3] C. J. Maggiore, A. M. Clogston, G. Spalek, W. C. Sailor, and F. M. Mueller, "Low-loss microwave cavity using layered-dielectric materials," *Applied Physics Letters*, vol. 64, no. 11, pp. 1451–1453, 03 1994.

[4] C. Flory and H. Ko, "Microwave oscillators incorporating high performance distributed bragg reflector microwave resonators," *IEEE Transactions on Ultrasonics, Ferroelectrics, and Frequency Control*, vol. 45, no. 3, pp. 824–829, 1998.

[5] C. Flory and R. Taber, "High Performance Distributed Bragg Reflector Mircowave Resonator," *IEEE Transactions On Ultrasonics, Ferroelectrics, and Frequency Control*, vol. 44, no. 2, pp. 468–495, 1997.

[6] J. Breeze, J. Krupka, and N. M. Alford, "Enhanced quality factors in aperiodic reflector resonators," *Appl. Phys. Lett*, vol. 91, no. 15, 2007.

[7] J. Breeze, M. Oxborrow, and N. McN Alford, "Better than Bragg: Optimizing the quality factor of resonators with aperiodic dielectric reflectors," *Applied Physics Letters*, vol. 99, no. 11, p. 113515, 09 2011.

[8] S. Bale and J. Everard, "High-Q X-Band Distributed Bragg Resonator Utilizing an Aperiodic Alumina Plate Arrangement," *IEEE Transactions On Ultrasonics, Ferroelectrics, and Frequency Control*, vol. 57, no. 1, pp. 66–73, 2010.

[9] S. J. Bale, P. D. Deshpande, M. Hough, S. J. Porter, and J. K. A. Everard, "High-q tuneable 10-ghz bragg resonator for oscillator applications," *IEEE Transactions on Ultrasonics, Ferroelectrics, and Frequency Control*, vol. 65, no. 2, pp. 281–291, 2018.

[10] J. Everard, M. Xu, and S. Bale, "Simplified phase noise model for negative-resistance oscillators and a comparison with feedback oscillator models," *IEEE Transactions on Ultrasonics, Ferroelectrics, and Frequency Control*, vol. 59, no. 3, pp. 382–390, 2012.

[11] K. K. M. Cheng and J. K. A. Everard, "Noise performance degradation in feedback oscillators with nonzero phase error," *Microw. Opt. Technol. Lett.*, vol. 4, no. 2, pp. 64–66, Jan. 1991.

[12] R. Boudot and E. Rubiola, "Phase noise in RF and microwave amplifiers," *IEEE Trans. Ultrason. Ferroelectr. Freq. Control*, vol. 59, no. 12, pp. 2613–2624, Dec. 2012.

[13] S. J. Bale, D. Adamson, B. Wakley, and J. Everard, "Cross correlation residual phase noise measurements using two hp3048a systems and a pc based dual channel fft spectrum analyser," in *EFTF-2010 24th European Frequency and Time Forum*, 2010, pp. 1–8.